Carcinogenesis, 2021, Vol. 42, No. 1, 136–147

doi:10.1093/carcin/bgaa085
Advance Access publication July 25, 2020
Original Article

ORIGINAL ARTICLE

Downregulation of hedgehog-interacting protein (HHIP) contributes to hexavalent chromium-induced malignant transformation of human bronchial epithelial cells

Peichao Li[1,2], Xiaoru Zhang[2], Anthony J. Murphy[2], Max Costa[2], Xiaogang Zhao[1,*] and Hong Sun[2,*]

[1]Department of Thoracic Surgery, The Second Hospital, Cheeloo College of Medicine, Shandong University, Jinan, Shandong, 250012, China and [2]Department of Environmental Medicine, NYU School of Medicine, New York 10010

*To whom correspondence should be addressed. Tel: 1-(646) 754 9459; Fax: 1-(646) 754 9448; Email: Hong.sun@nyumc.org
Correspondence may also be addressed to Xiaogang Zhao. Tel: 86-531-85875009; Fax: 86-531-88962544; Email: zhaoxiaogang@sdu.edu.cn

Abstract

Hexavalent chromium [Cr(VI)] is a potent human lung carcinogen. Multiple mechanisms have been proposed that contribute to Cr(VI)-induced lung carcinogenesis including oxidative stress, DNA damage, genomic instability and epigenetic modulation. However, the molecular mechanisms and pathways mediating Cr(VI) carcinogenicity have not been fully elucidated. Hedgehog (Hh) signaling is a key pathway that plays important roles in the formation of multiple tissues during embryogenesis and in the maintenance of stem cell populations in adults. Dysregulation of Hh signaling pathway has been reported in many human cancers. Here, we report a drastic reduction in both mRNA and protein levels of hedgehog-interacting protein (HHIP), a downstream target and a negative regulator of Hh signaling, in Cr(VI)-transformed cells. These findings point to a potential role of Hh signaling in Cr(VI)-induced malignant transformation and lung carcinogenesis. Cr(VI)-transformed cells exhibited DNA hypermethylation and silencing histone marks in the promoter region of *HHIP*, indicating that an epigenetic mechanism mediates Cr(VI)-induced silencing of *HHIP*. In addition, the major targets of Hh signaling (GLI1-3 and PTCH1) were significantly increased in Cr(VI)-transformed cells, suggesting an aberrant activation of Hh signaling in these cells. Moreover, ectopically expressing HHIP not only suppressed Hh signaling but also inhibited cell proliferation and anchorage-independent growth in Cr(VI)-transformed cells. In conclusion, these findings establish a novel regulatory mechanism underlying Cr(VI)-induced lung carcinogenesis and provide new insights for developing a better diagnostic and prognostic strategy for Cr(VI)-related human lung cancer.

Introduction

Lung cancer is the leading cause of cancer death for both men and women in the United States. In 2020, approximately 228,820 new lung cancer cases and 135,720 lung cancer deaths are projected according to the American Cancer Society (1). Non-small cell lung cancers (NSCLC), including lung adenocarcinoma (LUAD), lung squamous cell carcinoma (LUSC) and large cell carcinoma, account for approximately 85% of all lung cancer diagnoses (2). Despite significant improvements in early diagnosis, surgical advances and chemo-radiotherapy in the past decades, the prognosis of patients with lung cancer remains very poor, with a 5-year survival rate less than 20% (1). Elucidating the factors that contribute to lung carcinogenesis and identifying the genes and molecules involved are of particular importance.

Hexavalent chromium [Cr(VI)] is a well-established human lung carcinogen (3,4). Due to its extensive use in many industrial processes, including chrome pigment production, chrome

Received: June 4, 2020; **Revised:** July 10, 2020; **Accepted:** July 20, 2020

Abbreviations

5-AZA	5-aza-2-deoxycytidine
DEG	differentially expressed gene
GLI	glioma-associated oncogene homolog
HHIP	Hedgehog-interacting protein
LUAD	lung adenocarcinoma
LUSC	lung squamous cell carcinoma
NHBE	normal human bronchial epithelial
NSCLC	non-small cell lung cancer
PBS	phosphate buffered solution
PTCH	Patched homolog
SHH	sonic hedgehog
SMO	smoothened

plating, stainless steel manufacturing, leather tanning, etc., occupational exposure to Cr(VI) possess a high risk of lung cancer (5,6). Epidemiological studies have reported high incidences of lung cancer among chromate workers chronically exposed to Cr(VI) through inhalation. The International Agency for Research on Cancer classified Cr(VI) as a class I human carcinogen when exposed through inhalation (7). Multiple mechanisms have been shown to contribute to Cr(VI)-induced lung carcinogenesis, including oxidative stress, DNA damage, genomic instability and epigenetic modulation (8,9); however, the molecular mechanisms and downstream genes mediating chromium carcinogenicity have not yet been fully elucidated.

To investigate the potential mechanisms and molecules contributing to Cr(VI)-induced lung carcinogenesis, we established several Cr(VI)-transformed cell lines by subchronically exposing immortalized human bronchial epithelial BEAS-2B cells to low doses of Cr(VI) followed by selection based on anchorage-independent growth ability (10). Gene expression profiling of Cr(VI)-transformed cells revealed 409 differentially expressed genes (DEGs) compared with control cells. Hedgehog-interacting protein (HHIP), an important negative regulator and a downstream target gene in the hedgehog (Hh) signaling pathway, was among the top 20 DEGs, suggesting the possible involvement of HHIP and Hh signaling in Cr(VI)-induced cell transformation (10).

Hh signaling plays important roles in embryonic development and stem cell self-renewal (11,12). The signaling cascade is initiated by the binding of Hh ligands to their receptors on the plasma membrane (13). Three mammalian Hh ligands, sonic hedgehog (SHH), Indian hedgehog and desert hedgehog, can bind to the same receptor and elicit a similar response. Hh receptors, Patched-homolog 1 and 2 (PTCH 1 and 2), are normally associated with the G protein-coupled receptor Smoothened (SMO), and inhibit SMO's activity in the absence of Hh ligand. Binding of Hh ligands to PTCH alters the interaction between PTCH and SMO, resulting in the activation of SMO, which in turn leads to the nuclear translocation of glioma-associated oncogene homolog (GLI) transcription factors. Once entering the nucleus, GLI binds to the DNA and activates a series of Hh target genes. HHIP is a membrane glycoprotein that binds to Hh ligands with an affinity similar to that of the Hh receptor PTCH1 (14). Unlike PTCH1, HHIP lacks signal transduction capacity and is not able to activate SMO and downstream signaling. HHIP inhibits Hh signaling by binding and sequestering all three hedgehogs on the cell surface. In addition, HHIP itself is a transcriptional target of Hh signaling (14). Activation of the Hh signaling pathway may lead to an increased level of HHIP that functions as an inducible antagonist of Hh to reduce the intensity of Hh signaling.

In the adult lung, Hh signaling is limited to the airway epithelial progenitor (stem) cells and is crucial for the maintenance and the expansion of these cells (15). Active Hh signaling has been reported in both NSCLC and small cell lung cancers (16–18). Two recent studies reported an important role of Hh signaling pathway in the survival and progression of lung cancer cells, and ectopic expression of HHIP suppressed proliferation, migration and invasion of NSCLC cells (19,20).

Our previous study revealed reduced HHIP expression in Cr(VI)-transformed cells, suggesting a potential role of HHIP and Hh signaling in Cr(VI)-induced malignant transformation and lung carcinogenesis. The primary focus of the current study was to determine the role of HHIP in Cr(VI)-induced cell transformation and to dissect the mechanism by which Cr(VI) modulates HHIP expression. Our results demonstrate that Cr(VI) downregulates HHIP expression via promoter hypermethylation, which subsequently leads to aberrant activation of Hh signaling and enhanced anchorage-independent growth, eventually contributing to Cr(VI)-induced malignant transformation of human lung cells.

Materials and methods

Cell culture

Human bronchial epithelial BEAS-2B cells (ATCC®_CRL-9609) were maintained in Dulbecco's modified Eagle's medium supplemented with 10% fetal bovine serum and 1% Pen Strep. Cells were authenticated by STR DNA profiling (Genetica) before experiments were initiated. Normal human bronchial epithelial (NHBE) cells were obtained from Lonza (CC-2541) and were maintained according to the manufacturer's instruction. Cr(VI)-transformed BEAS-2B cell lines were established as previously described (10). Cr(VI)-transformed cells stably expressing Myc-tagged HHIP were established by transfecting pCMV6-HHIP (Origene, RC206868) using lipofectamine LTX reagent (Thermo Fisher Scientific, 15338030) and selected with 800 μg/ml G418 (Thermo Fisher Scientific, 10131035). For acute Cr(VI) exposure, cells were treated with various doses of potassium chromate (K_2CrO_4, Sigma, 216615) for 48 h. All cells were maintained at 37°C in a humidified incubator containing 5% CO_2.

RNA isolation and reverse transcription-quantitative PCR

Total RNA was extracted from cells using TRI Reagent (MRC, TR 118) following the manufacturer's instructions. The concentration of total RNA was measured with NanoDrop 2000 spectrophotometer (Thermo Fisher Scientific). 0.5 μg of total RNA was reverse-transcribed into first-strand cDNA using LunaScript™ RT SuperMix Kit (NEB, E3010). Quantitative real-time PCR were performed on QuantStudio™ 6 Flex System (Thermo Fisher Scientific) using Power SYBR® Green Master Mix (Thermo Fisher Scientific, 4367659). Relative gene expression level, normalized to β-actin, was calculated using $2^{-\Delta\Delta CT}$ method. The primers of HHIP and Hh signaling components are listed in Supplementary Table 1, available at *Carcinogenesis* Online. All PCRs were performed in triplicate. The results were presented as fold change relative to the level in controls.

Western blot analysis

Cells were washed twice with cold phosphate buffer solution (PBS) and lysed with RIPA buffer (CST, 9806) for 30 min on ice. Protein concentrations were measured using DC Protein Assay Kit II (Bio-Rad, 5000112). About 50 μg of protein lysates were separated by sodium dodecyl sulfate–polyacrylamide gel electrophoresis and transferred to nitrocellulose membranes (Bio-Rad, 1620115). Nonspecific binding sites were blocked in Tris-buffered saline buffer containing 5% nonfat milk for one hour at room temperature, followed by incubation with primary antibodies (Supplementary Table 2, available at *Carcinogenesis* Online) overnight at 4°C. Membranes were then incubated in horseradish peroxidase conjugated secondary antibody solution at room temperature for 1 h. The signal was detected using an enhanced chemiluminescent substrate (Thermo Fisher Scientific, 32106). β-Actin was used as an internal loading control.

Immunofluorescence

Cells were seeded in eight-chamber culture slides (Lab-Tek™ II, Thermo Fisher Scientific, 154534) at 7500 cells per chamber. 16–24 Hours later, cells were fixed with 4% paraformaldehyde for 10 min at room temperature. After washing with PBS three times, the cells were blocked with PBS containing 5% bovine serum albumin for 1 h at room temperature. Cells were incubated with primary antibodies against Myc-Tag at 4°C overnight, and followed by incubation with Alexa Fluor 488-conjugated goat anti-mouse IgG (1:2000; Invitrogen, A11029) for one hour at room temperature in dark. The chamber slides were mounted with ProLong™ Diamond Antifade Mountant with DAPI (Invitrogen, P36962) and sealed with nail polish. The images were acquired using ZOE Fluorescent Cell Imager (Bio-Rad).

Cell proliferation

Cell proliferation was measured using MTS assay. Cells were seeded in 96-well plates at 2500 cells per well. MTS Reagent (Abcam, ab197010) was added each day and the cells were incubated for additional 3 h. The number of viable cells were determined by the absorbance at 490 nm using SpectraMax M2e Microplate reader (Molecular Devices). An initial absorbance was measured at 6 h after seeding cells, then absorbance was read every 24 h. The experiments were repeated three times and the data represented as the mean of quadruplicate wells ± SD.

Soft-agar assay

Cells were plated at 5000 cells per well in six-well plates with culture medium containing 0.35% low-melting-point agarose (Sigma, A4018) over a 0.5% agarose base layer and cultured at 37°C incubator with 5% CO_2 for 3 weeks. The colonies were stained with INT/BCIP (Roche, 11681460001) and photographed using Molecular Imager® Gel Doc™ XR+ System with Image Lab™ Software (Bio-Rad). The number of colonies was calculated with Image J (NIH). Data from three independent experiments were expressed as the mean of triplicate wells ± SD.

Chromatin immunoprecipitation assay

Cr(VI)-transformed cells were seeded in 150-mm culture dishes and cultured until reaching 80–90% confluence. Cells were crosslinked with 1% formaldehyde in the culture medium for 10 min at room temperature, and followed by incubation with 0.125 M Glycine for 5 min. After washing with ice-cold PBS, cells were harvested by scraping and resuspend in sonication buffer (10 mM Tris–HCl, pH 8.0; 1 mM ethylenediaminetetraacetic acid, 0.1% sodium dodecyl sulfate). Chromatin fragmentation was performed using Bioruptor XL water bath (Diagenode) for 25–30 min. Fragmented chromatin was then subjected to immunoprecipitation overnight at 4°C using antibodies against various histone modification (Supplementary Table 2, available at *Carcinogenesis* Online). Normal mouse and rabbit IgG were used as negative control. After extensive washes, precipitated chromatins were de-crosslinked in the presence of proteinase K for overnight at 65°C. DNA was purified by phenol/chloroform, precipitated by ethanol, and resuspended in water. Quantitative PCR was performed using primers for HHIP promoter (Supplementary Table 1, available at *Carcinogenesis* Online).

Methylation-specific PCR

Genomic DNA was isolated with the DNeasy Blood & Tissue Kit (Qiagen) according to the manufacturer's instruction. Bisulfite conversion of genomic DNA (2 μg) was performed using the EpiTect Bisulfite conversion Kit (Qiagen). About 20 ng of bisulfite-converted DNA was then subjected to methylation-specific PCR using the methylated primer and unmethylated primers for human HHIP promoter (Supplementary Table 1, available at *Carcinogenesis* Online) with the following condition: one initial cycle at 95°C for 10 min, 35 cycles of 95°C for 15 s, 55°C for 30 s and 72°C for 30 s, and a final extension cycle at 72°C for 10 min. PCR products were run on 1% agarose gel and visualized after ethidium bromide staining. Bisulfite-converted methylated and unmethylated DNA from EpiTect PCR Control DNA Set (Qiagen) were used as positive and negative controls.

Statistical analysis

Results from at least three independent experiments were expressed as mean ± SD. Significant difference between any two groups was determined by Student's *t*-test. *P*-values <0.05 were considered to be statistically significant. All of the data were analyzed and visualized using GraphPad Prism 7 (La Jolla, CA).

Results

HHIP is downregulated in Cr(VI)-transformed cells and human NSCLC samples

Our previous study identified 409 DEGs in Cr(VI)-transformed BEAS-2B cells compared with control cells. Among the top 20 DEGs, HHIP was downregulated about 12-fold in the transformed cells (10). To confirm that HHIP is indeed downregulated in Cr(VI)-transformed cells, total RNA was extracted from BEAS-2B cells and four Cr(VI)-transformed cell lines, and subjected to reverse transcription-quantitative PCR analysis. As shown in Figure 1A, the levels of HHIP were significantly reduced in all four Cr(VI)-transformed cells compared with normal BEAS-2B cells, suggesting that HHIP downregulation is a common phenotype shared by Cr(VI)-transformed cells. Downregulation of HHIP was further supported by remarkably reduced HHIP protein levels in Cr(VI)-transformed cells (Figure 1B). Moreover, Cr(VI)-transformed cells exhibited a significant increase in the number of colonies growing in soft agar compared with BEAS-2B cells, suggesting an enhanced capacity of anchorage-independent growth (Figure 1C and D). Therefore, our results indicate that Cr(VI)-transformed cells exhibit reduced HHIP expression at both mRNA and protein levels, accompanied by enhanced anchorage-independent growth.

Downregulation of HHIP has been reported in many cancers (19,21–24). Next, we explored HHIP expression changes in NSCLC tumor samples as well as the association between HHIP expression and survival of NSCLC patients using data obtained from The Cancer Genome Atlas. Analyzing RNA sequencing data of LUAD (tumor = 514, normal = 59) and LUSC (tumor = 502; normal = 51) revealed significantly reduced HHIP expression in primary tumors of both LUAD and LUSC compared with normal tissues (Figure 1E and F). However, despite the significant downregulation of HHIP expression in NSCLC tumors, no significant difference was found in overall survival and disease-specific survival between HHIP high- and low-expression groups in both LUAD and LUSC patients (Supplementary Figure 1, available at *Carcinogenesis* Online). Thus, HHIP expression was reduced in both Cr(VI)-transformed cells and primary lung cancers.

Promoter hypermethylation and histone modification contribute to HHIP downregulation in Cr(VI)-transformed cell lines

Downregulation of HHIP mRNA in many human cancers has been correlated with CpG hypermethylation in its promoter region (21,24–27). Therefore, we explored whether DNA methylation or histone modification mediated HHIP downregulation in Cr(VI)-transformed cells. Two Cr(VI)-transformed cell lines (Cr1, Cr4) were treated with DNA methylation inhibitor, 5-aza-2-deoxycytidine (5-AZA), or histone deacetylase inhibitor, trichostatin A (TSA), or a combination of 5-AZA and TSA. Interestingly, whereas 5-AZA or TSA treatment significantly increased HHIP mRNA levels in these cells, co-treatment of 5-AZA and TSA produced a greater effect (20- to 30-fold) on re-activation of HHIP transcription (Figure 2A). The results suggest that DNA methylation and histone deacetylation play important roles in silencing HHIP in Cr(VI)-transformed cells.

To further confirm that promoter hypermethylation is involved in Cr(VI)-induced HHIP downregulation, we examined

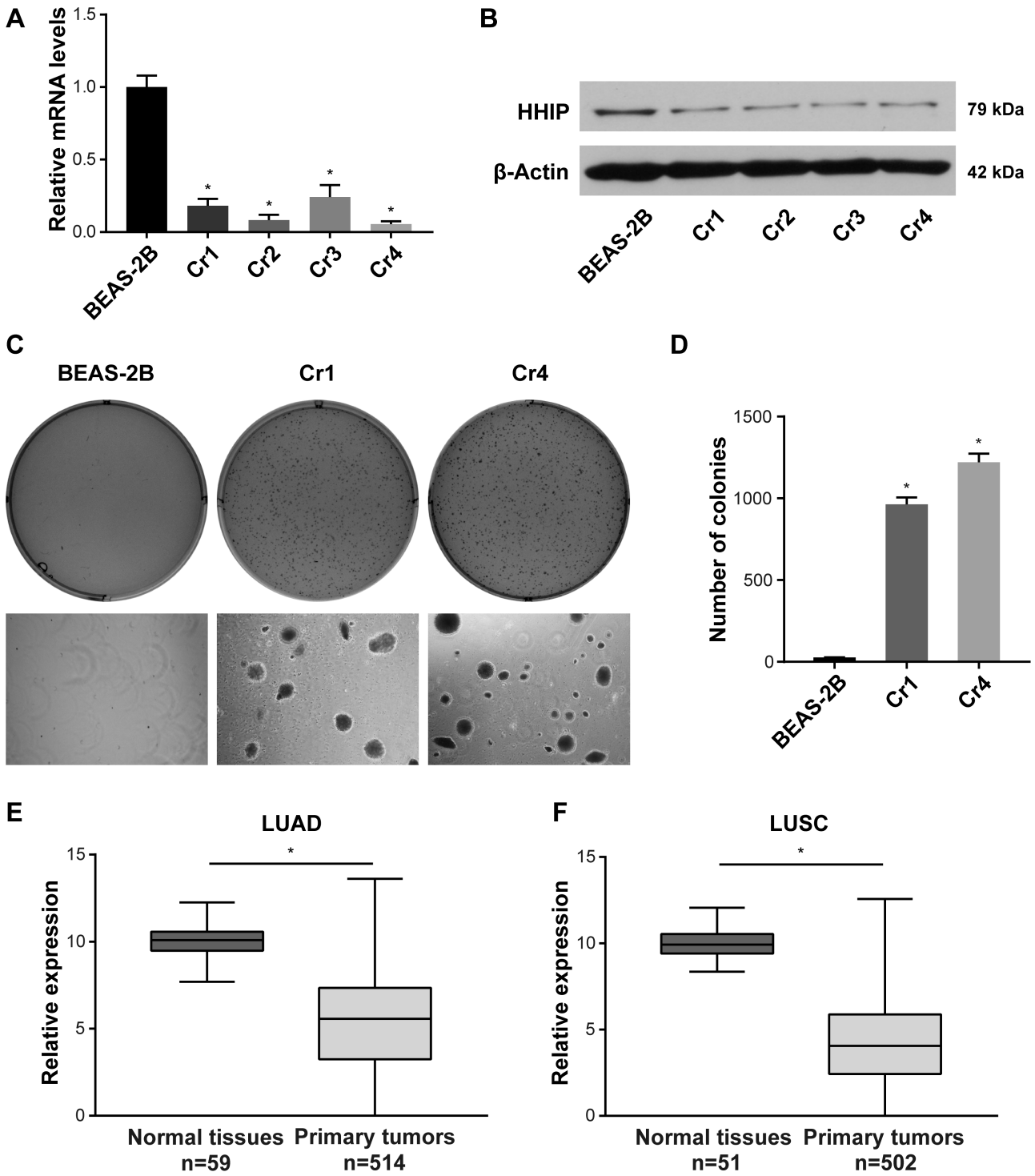

Figure 1. HHIP was reduced in Cr(VI)-transformed cells and primary lung tumors. **(A)** Total RNA was extracted from four Cr(VI)-transformed cell lines (Cr1-4) and BEAS-2B cells. Expression levels of HHIP mRNA were analyzed by reverse transcription-quantitative PCR, normalized to β-actin mRNA expression, and presented as relative fold change to the level expressed in BEAS-2B cells. Results are mean ± SD (n = 3). *P < 0.05. **(B)** Total protein lysate from BEAS-2B and Cr(VI)-transformed cells were analyzed by western blot using antibody against to HHIP. β-actin was used as a loading control. **(C** and **D)** Anchorage-independent growth of two Cr(VI)-transformed cell lines (Cr1,4) and BEAS-2B cells were assessed using soft agar assay. In total, 5000 cells were plated in each well of six-well plates. Cell colonies were stained with INT/BCIP and photographed after 3 weeks. **(C)** Representative images and partial enlarged details of soft agar plates were displayed. **(D)** Numbers of colonies were presented as the mean ± SD (n = 3). *P < 0.05. **(E and F)** LUAD and LUSC data sets from The Cancer Genome Atlas were used to determine mRNA level of HHIP in lung tumor samples (514 samples in LUAD and 502 samples in LUSC) and normal tissues (59 samples in LUAD and 51 samples in LUSC). Expression of HHIP was analyzed in log2 (RSEM normalized count + 1). Results are presented as means ± SD. *P < 0.05

the methylation state of the HHIP promoter using methylation-specific PCR. A CpG island located in the region proximal to HHIP transcription starting site, spanning ~1 kb and containing 91 CpG sites, was used to assess HHIP promoter hypermethylation. As shown in Figure 2B, whereas BEAS-2B cells predominantly generated unmethylated PCR product

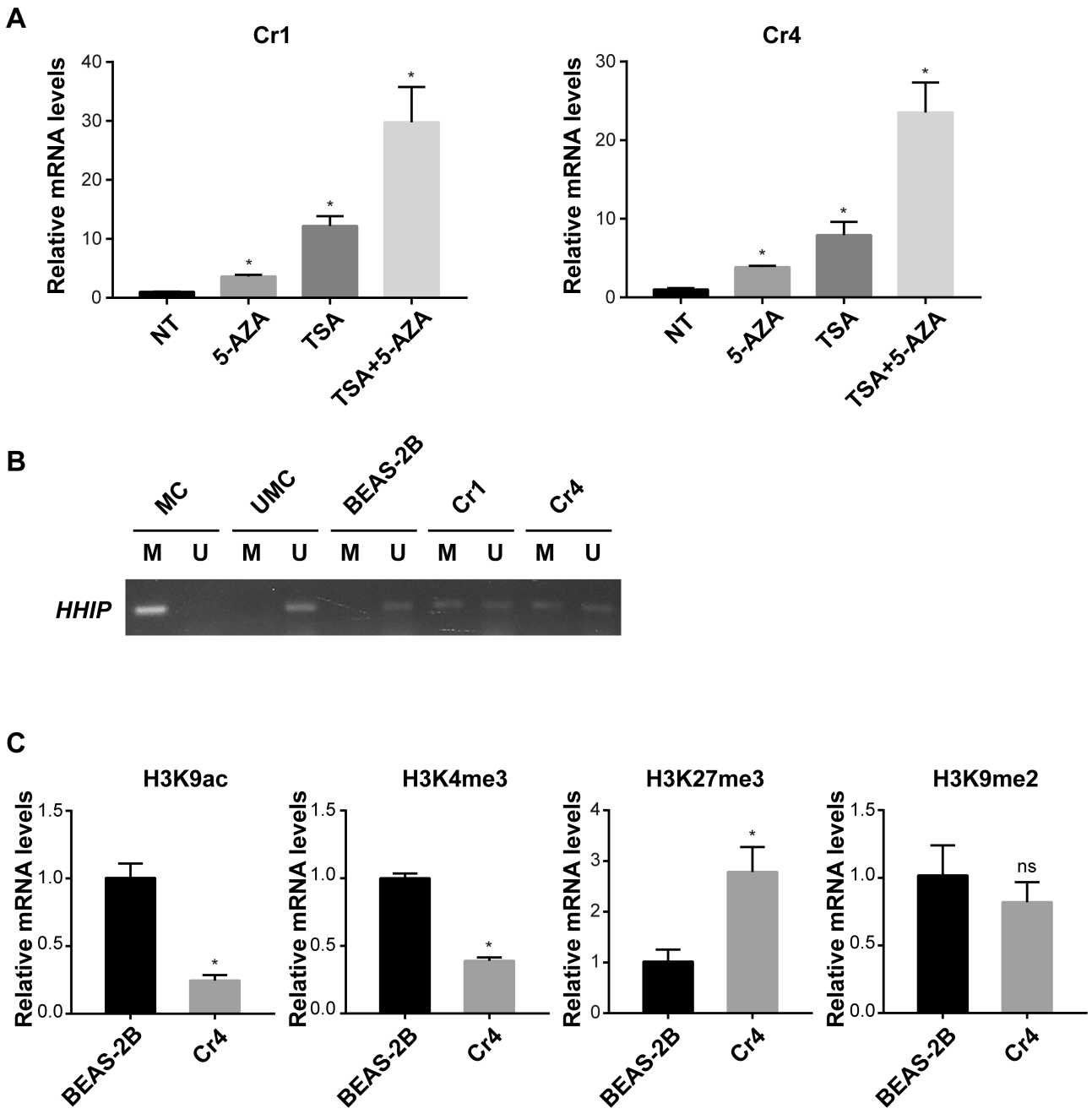

Figure 2. Cr(VI) downregulated HHIP by promoter methylation and histone modification. **(A)** Re-activation of HHIP mRNA expression by Trichostatin A (TSA) and 5-AZA in Cr(VI)-transformed cells. Cell were treated with 5 μM 5-AZA for 48 h or 0.5 μM TSA for 8 h, or combined 5-AZA and TSA. HHIP mRNA expression was measured by reverse transcription-quantitative PCR. The results were normalized to β-actin mRNA expression, and presented as relative fold change to samples with no treatment (NT). Data are mean ± SD ($n = 3$). *$P < 0.05$. **(B)** Increased DNA methylation in HHIP gene promoter on Cr(VI)-transformed cells. Genomic DNA was extracted from BEAS-2B, Cr1, and Cr4 cells. Methylation specific PCR was performed using bisulfite converted DNA and the primers specific to methylated (M) or unmethylated (U) HHIP promoter. EpiTect control DNA kit was used as positive (MC) and negative controls (UMC). **(C)** Chromatin immunoprecipitation was performed in Cr(VI)-transformed cells (Cr4) using antibodies against active histone marks (H3K9ac and H3K4me3) and repressive marks (H3K27me3 and H3K9me2). The levels of each histone mark in the HHIP promoter were measured by ChIP-qPCR, and normalized to the input DNA. *$P < 0.05$; ns means no significance.

(188 bp), two Cr(VI)-transformed cells (Cr1 and Cr4) generated both unmethylated and methylated (190 bp) PCR products, suggesting HHIP promoter is partially methylated in these cells.

Chromatin immunoprecipitation was performed to examine the changes of histone modification in HHIP promoter using antibodies against two active histone marks (H3K9ac and H3K4me3) and two repressive histone marks (H3K9me2 and H3K27me3). Consistent with reduced HHIP expression, H3K27me3 was significantly enriched in the HHIP promoter region in Cr(VI)-transformed cells, accompanied by reduced levels of H3K9ac and H3K4me3 (Figure 2C). Surprisingly, another repressive mark, H3K9me2, displayed no significant difference between Cr(VI)-transformed cells and BEAS-2B cells (Figure 2C). Taken together, these results suggest that an epigenetic mechanism mediates Cr(VI)-induced HHIP downregulation.

Dysregulation of Hedgehog signaling pathway in Cr(VI)-transformed cells

HHIP has been identified to be a downstream target and a natural antagonist of Hedgehog signaling (14). HHIP downregulation in Cr(VI)-transformed cells could implicate either the inactivation (as a Hh target gene) or activation (as an antagonist) of Hh signaling pathways. To assess endogenous Hh activity, we analyzed the mRNA levels of the major components of Hh signaling, including SHH, SMO, GLI1-3 and PTCH1 in two Cr(VI)-transformed cell lines. Expression levels of Hh target genes GLI1 and PTCH1 are considered to be the most reliable markers for Hh pathway activity (13,28). As shown in Figure 3A, the mRNA levels of GLI1-3 and PTCH1 displayed small but significant increases in Cr(VI)-transformed cells compared with BEAS-2B cells, whereas no significant change was detected in SHH and SMO mRNA expression. Increased expression of Hh target genes indicated enhanced Hh signaling in Cr(VI)-transformed cells.

It has been reported that, in adult lung, Hh signaling is limited to the airway epithelial progenitor (stem) cells (15). Therefore, we reasoned that the small changes of endogenous Hh target genes may be due to rather limited Hh activity in these cells. It is known that serum starvation increases the number and length of primary cilia and activates Hh signaling (29–31). To test whether Cr(VI)-transformed cells response differently to Hh signaling activated by serum starvation, BEAS-2B and two Cr(VI)-transformed cell lines were placed in medium containing reduced serum (1 and 0.1%) and analyzed for expression of Hh targets. Interestingly, whereas BEAS-2B cells showed slightly increased GLI1 (~2-fold) and PTCH1 (~1.5-fold) mRNA levels in low serum medium, two Cr(VI)-transformed cells exhibited significant increases in both GLI1 (~5 to 9-fold) and PTCH1 (~2 to 2.5-fold) expression, suggesting Hh signaling is less suppressed in these cells (Figure 3B). In addition, analyzing SHH expression in Cr(VI)-transformed cells revealed an increased SHH mRNA in serum-starved cells (Supplementary Figure 2, available at *Carcinogenesis* Online).

In order to rule out the possibility that Cr(VI) exposure directly activates Hh signaling, BEAS-2B and NHBE cells were exposed to various doses of Cr(VI) for 48 h, and the expression of GLI1, PTCH1 and HHIP mRNA were analyzed by reverse transcription-quantitative PCR. As shown in Figure 4A and B, GLI1 mRNA was significantly reduced at the higher dose in both BEAS-2B (2 μM group) and NHBE cells (5 μM group), whereas reduction of PTCH1 and HHIP mRNA was significant only in BEAS-2B but not in HNBE cells. The reduced Hh activity in Cr(VI)-treated BEAS-2B cells was further supported by the luciferase reporter assay using a GLI reporter construct containing tandem repeats of the GLI transcriptional response element upstream of the minimal promoter and the luciferase gene (data not shown).

Taken together, our results indicate that downregulation of HHIP in Cr(VI)-transformed cells is not the consequence of Hh inhibition but rather the cause for the aberrant activation of Hh signaling pathway in these cells.

Ectopic expression of HHIP in Cr(VI)-transformed cells inhibited Hh signaling and reduced cell proliferation and anchorage-independent growth

To determine whether downregulation of HHIP and subsequent dysregulation of Hh pathway contribute to Cr(VI)-induced cell transformation, we ectopically expressed HHIP in Cr(VI)-transformed cells. The plasmids containing myc-tagged human HHIP cDNA or empty vector were transfected into Cr(VI)-transformed cells (Cr4). Stable transfectants expressing either HHIP (Cr4-HHIP) or empty vector (Cr4-EV) were established. Expression of HHIP mRNA and protein were verified by reverse transcription-quantitative PCR and western blot analysis (Figure 5A and B). Immunofluorescence staining revealed that exogenous HHIP protein was mainly located in plasma membrane (Figure 5C). Analyzing the expression of Hh targets revealed a reduced GLI1 and GLI2 levels in HHIP expressing cell compared with those with empty control (Figure 5D). These results suggest that aberrantly activated Hh signaling in Cr(VI)-transformed cells was reversed by ectopic expression of HHIP.

The activation of Hh signaling pathway has been reported to be crucial to cell survival and stemness. Thus, we assessed cell proliferation of Cr(VI)-transformed cells stably expressing HHIP using MTS assay. As shown in Figure 6A, cell expressing empty vector exhibited accelerated cell proliferation compared with BEAS-2B cells, whereas cells expressing HHIP displayed a markedly reduced proliferation rate. Consistent with reduced cell proliferation, cells ectopically expressing HHIP exhibited a significant reduction in anchorage-independent growth (Figure 6B and C). Taken together, ectopic expression of HHIP in Cr(VI)-transformed cells not only inhibited aberrant Hh activity but also reduced cell proliferation and anchorage-independent growth.

Discussion

Cr(VI) is a well-established human lung carcinogen (3,4). However, the molecular mechanisms and pathways mediating Cr(VI) carcinogenicity are not fully elucidated. In the present study, we uncovered a new mechanism by which subchronic Cr(VI) exposure induced DNA hypermethylation and histone modification in the HHIP promoter region, leading to downregulation of HHIP and aberrant activation of Hh signaling. This facilitated cell proliferation and anchorage-independent growth, eventually contributing to Cr(VI)-induced cell transformation (Figure 6D).

In an attempt to identify new genes and pathways mediating Cr(VI) carcinogenicity, we previously established several transformed cell lines by subchronic exposure of BEAS-2B cells to low doses of Cr(VI) (10). These transformed cells not only exhibited an accelerated cell growth but also displayed the ability to form tumor xenografts in nude mice. Among 409 DEGs identified by Affymetrix Genechip analysis, HHIP is one of the top downregulated genes in Cr(VI)-transformed cells compared with controls (10). In this study, we verified HHIP expression in Cr(VI)-transformed and parental BEAS-2B cells at both mRNA and protein levels. Consistent with microarray data, the levels of HHIP were significantly reduced in all of Cr(VI)-treated clones, compared with untreated BEAS-2B cells, suggesting that HHIP downregulation is a common phenotype shared by Cr(VI)-transformed cells. These results prompted us to examine HHIP expression in human lung tumors. Further analyzing RNA-seq data from The Cancer Genome Atlas database revealed significantly reduced HHIP expression in both LUAD and LUSC. Downregulation of HHIP in LUAD was further supported by two recent studies (19,20). Lin et al. analyzed a total of 85 pairs of LUAD samples and adjacent normal tissues obtained from two GEO datasets (GSE19804 and GSE27262) (19). While HHIP mRNA was significantly reduced in tumor tissues, expression of other components of Hh pathway was basically unchanged. In addition, five out of six LUAD cell lines exhibited reduced HHIP mRNA and protein expression compared with normal lung cell lines, which is in agreement with our finding of HHIP downregulation in Cr(VI)-transformed cell lines (19). It is worth noting that HHIP is similarly downregulated in LUSC, and the majority of lung cancers in chromate workers are LUSC

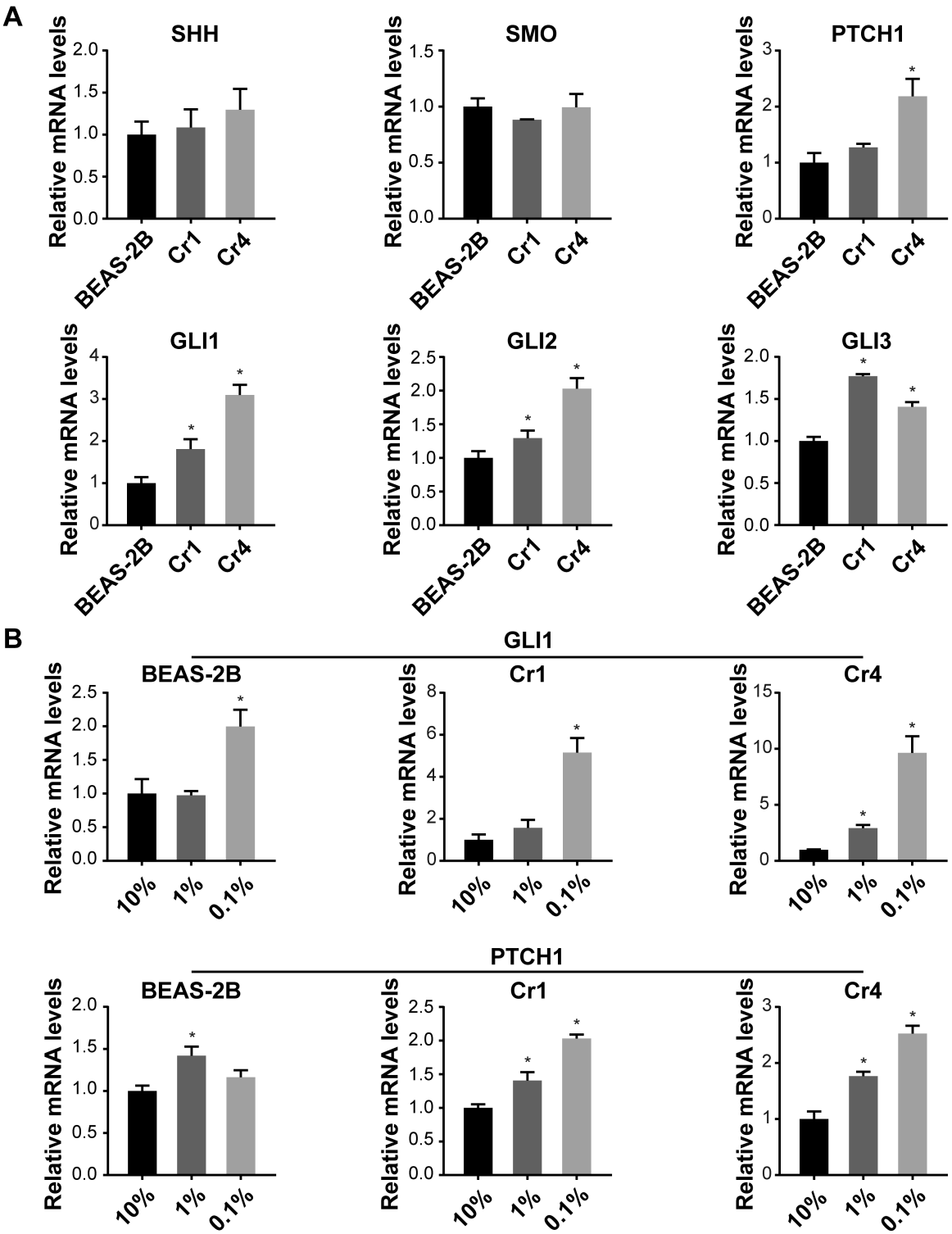

Figure 3. Dysregulation of hedgehog signaling pathway in Cr(VI)-transformed cells. **(A)** Total RNA was extracted from BEAS-2B cells and two Cr(VI)-transformed cell lines (Cr1, 4). Expression of SHH, SMO, PTCH1, GLI1, GLI2 and GLI3 mRNA were assessed using reverse transcription-quantitative PCR. The results were normalized to β-actin mRNA expression, and presented as mean ± SD (n = 3). *P < 0.05. **(B)** BEAS-2B cells and Cr(VI)-transformed cells (Cr1, 4) were treated with different concentrations of FBS (10, 1 and 0.1%) for 48 h. Expression of Hh downstream targets GLI1 and PTCH1 was analyzed using reverse transcription-quantitative PCR. The results were normalized to β-actin mRNA expression, and presented as relative fold change compared with cells treated with 10% FBS. Data are mean ± SD (n = 3). *P < 0.05.

(32). Given the fact that HHIP is both a downstream target and a negative inhibitor of Hh signaling, its downregulation in Cr(VI)-transformed cells and NSCLC tissues suggest a potential role of Hh signaling in Cr(VI)-induced cell transformation and lung carcinogenesis.

Reduced HHIP expression could indicate either a less active Hh signaling (as a Hh downstream target gene) or an enhanced Hh activity (as a natural Hh antagonist). Our analysis clearly revealed active Hh signaling in Cr(VI)-transformed cells, suggesting that HHIP acts as a Hh inhibitor. The basal levels of Hh

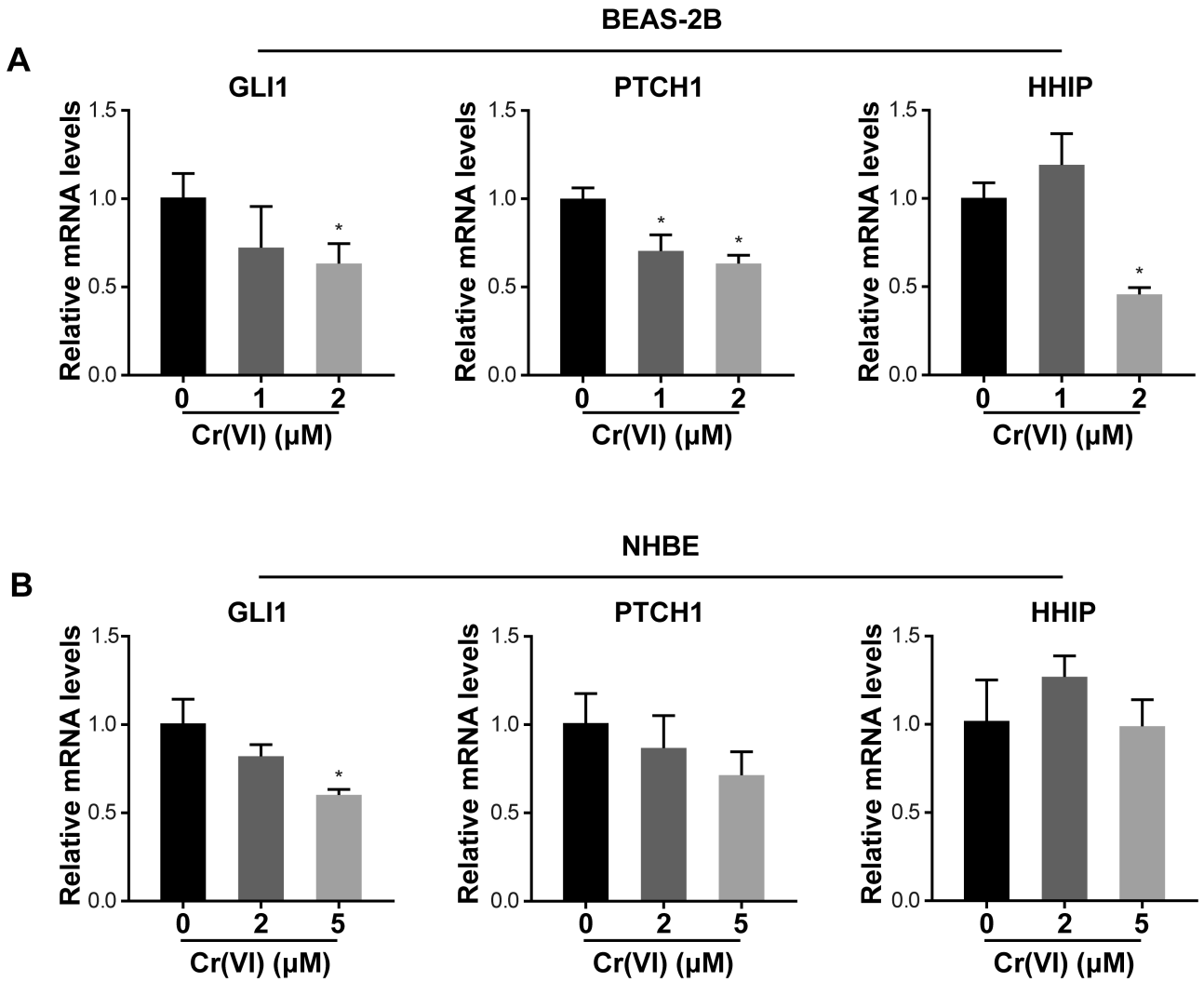

Figure 4. Changes of hedgehog signaling pathway in cells acutely exposed to Cr(VI). BEAS-2B **(A)** and normal human bronchial epithelia (NHBE) cells **(B)** were exposed to various doses of Cr(VI) for 48 h. Expression of Hh downstream targets (GLI1, PTCH1, HHIP) was analyzed using reverse transcription-quantitative PCR. Data were normalized to β-actin mRNA expression. Results were mean ± SD (n = 3) and shown as relative fold change compared with expression levels of untreated control. *$P < 0.05$.

target genes are higher in Cr(VI)-transformed cells compared with BEAS-2B cells, indicating enhanced Hh basal activity. In addition, when Hh signaling was measured in serum-starved cells, induced fold changes of GLI1 and PTCH1 mRNA were significantly increased in Cr(VI)-transformed cells compared with BEAS-2B cells, suggesting a relatively more sensitive Hh signaling in cells with reduced HHIP protein. Moreover, ectopically expressing HHIP in Cr(VI)-transformed cells inhibited Hh activity as evidenced by reduced expression of Hh downstream targets. Furthermore, acute exposure of BEAS-2B and NHBE cells to Cr(VI) failed to activate Hh signaling, further supporting that aberrant Hh activity in Cr(VI)-transformed cells is likely due to reduced HHIP. It remains unclear how HHIP downregulation lead to enhanced Hh signaling. Given the fact that HHIP is able to bind all Hh ligands and functions as a negative regulator of Hh signaling, our results suggest that downregulation of HHIP may result in an increased binding of Hh ligand to its receptor and subsequently lead to enhanced Hh signaling in Cr(VI)-transformed cells. Indeed, increased SHH expression has been reported in NSCLC tissues compared with adjacent normal tissue at both mRNA and protein levels (33–35). Results from other groups and our study indicated that serum starvation increased SHH mRNA expression in LUAD cells (19) and Cr(VI)-transformed cells. Further investigation will need to be conducted in order to verify whether NSCLC cells and Cr(VI)-transformed cells secrete SHH ligands. It is possible that both SHH upregulation and HHIP downregulation contribute to aberrant Hh signaling in NSCLC and Cr(VI)-transformed cells.

It has been reported that ligand-dependent activation of Hh signaling played an important role in maintaining a malignant phenotype in a subset of small cell lung cancer (17). Several studies reported upregulation of canonical Hh pathway components in both NSCLC tumor samples and cell lines (16,18,36), whereas others claimed negative or weak expression of these components in primary NSCLC tumors (19,33). Our novel findings of enhanced basal Hh activity and prompted activation of Hh signaling upon stress in Cr(VI)-transformed cells further support the involvement of aberrant Hh activity in malignant transformation.

Several studies have reported the effect of ectopic HHIP expression in different cancer cells (19,20,23,37,38). Similar to our observation, forced expression of HHIP in hepatoma

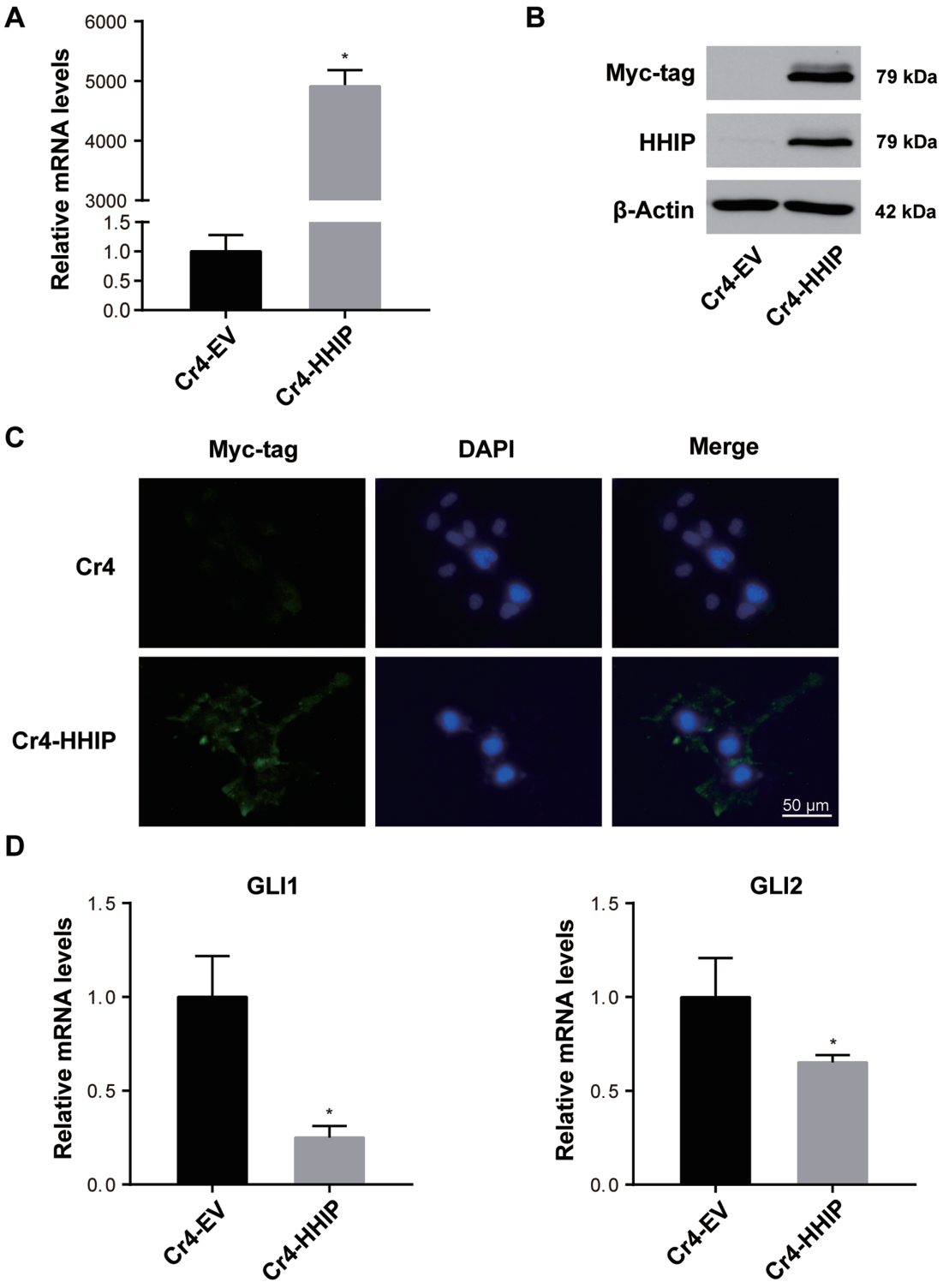

Figure 5. Ectopically expressing HHIP reversed the aberrant activation of Hh signaling pathway in Cr(VI)-transformed cells. Cr(VI)-transformed cells (Cr4) were transfected with pCMV6-HHIP and control vector plasmids, and selected for stable transfectants. **(A)** Total RNA was extracted from cells stably expressing HHIP (Cr4-HHIP) and its control vector (Cr4-EV) cells. HHIP mRNA expression was detected by reverse transcription-quantitative PCR, and normalized to β-actin mRNA expression. Results were presented as relative fold change to the expression level of Cr4-EV cells. Results are mean ± SD (n = 3). *P < 0.05. **(B)** Expression of HHIP protein was determined by western blot using antibody specifically against Myc-tag and HHIP. β-Actin was served as the loading control. **(C)** Cells were seeded in eight-chamber culture slides and analyzed for ectopic HHIP expression by immunofluorescent staining using antibody against Myc-tag. **(D)** Expression of Hh target genes GLI1 and GLI2 were determined by reverse transcription-quantitative PCR and normalized to mRNA expression of β-actin. Results were presented as relative fold change to Cr4-EV cells. Data were mean ± SD (*n* = 3). *P < 0.05.

HuH7 and Hep3B cells attenuated basal Hh activity, as evidenced by 30–40% reduction of GLI reporter activity and an approximate 40% reduction in basal levels of Hh target genes (23). Interestingly, in agreement with our observation of reduced cell proliferation in Cr4-HHIP cells, hepatoma cells expressing HHIP showed 40% growth reduction relative to control

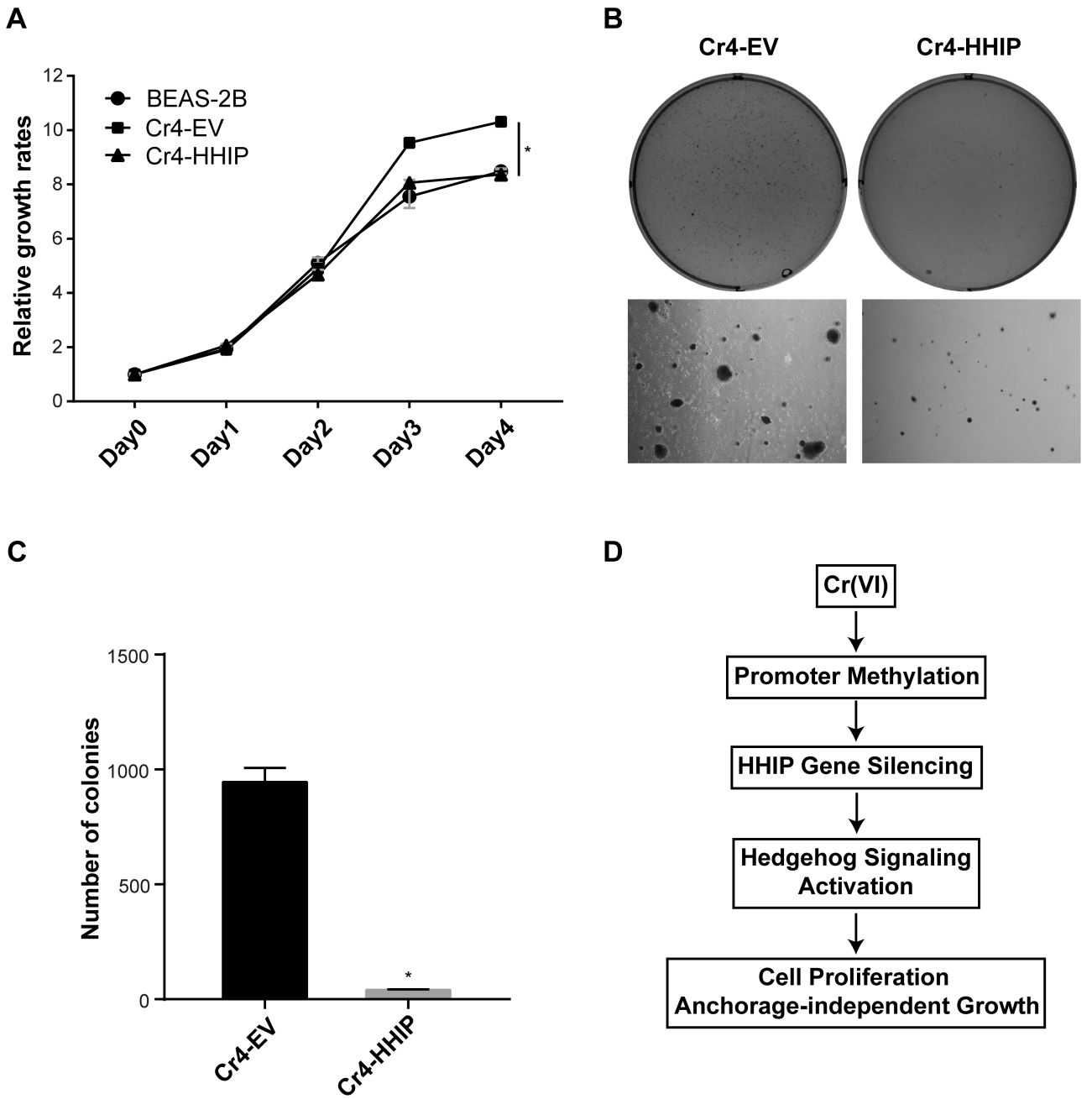

Figure 6. Expressing HHIP in Cr(VI)-transformed cells suppressed cell proliferation and anchorage-independent growth. **(A)** Cr4-EV, Cr4-HHIP and BEAS-2B cells were seeded at 2500 cells per well in 96-well plates. Cell proliferation was assessed via MTS assay at the indicated time point. Results were mean ± SD (n = 4). **(B** and **C)** Anchorage-independent growth of Cr4-EV and Cr4-HHIP cells was evaluated via a soft agar assay. (B) Representative images and partial enlarged details in soft agar assay were shown. (C) Numbers of colonies were mean ± SD (n = 3). *$p < 0.05$. **(D)** A schematic diagram indicated possible mechanisms underlying the potential function of HHIP silencing on cell proliferation and anchorage-independent growth in Cr(VI)-transformed cells.

cells, suggesting a crucial role of HHIP in growth inhibition (23). A similar growth inhibitory effect of HHIP has been reported in two recent studies on NSCLC. Zhao et al. reported that HHIP overexpression in HCC827 and H1975 lung adenocarcinoma cells inhibited cell proliferation, migration and invasion (20), whereas Lin et al. reported that overexpressing HHIP in the same lung adenocarcinoma cells significantly inhibited cell proliferation and invasion under stress condition such as serum starvation (19). In addition, when they were cultured in serum-free Matrigel, HHIP overexpressing cells formed fewer spheroids compared with control cells (19). Similarly, our results showed that ectopically expressing HHIP nearly abolished anchorage-independent growth of Cr(VI)-transformed cells. The ability to grow and form colonies in semisolid media (Matrigel or soft-agar) is considered as an important marker for tumorigenic and metastatic potential (39,40). Consistently, forced expression of HHIP in gastric cancer cell lines inhibited cell migration and invasion *in vitro* (37,38). Thus, repression of HHIP expression to facilitate anchorage-independent growth may be a prerequisite for malignant transformation and tumor progression, which is supported by HHIP downregulation in many human cancers.

It is not clear how HHIP is downregulated in Cr(VI)-transformed cells. Our study suggests an epigenetic mechanism mediating Cr(VI)-induced HHIP silencing. Highly repressed HHIP gene expression in transformed cells was reactivated by 5-AZA and TSA, the inhibitors of DNA methyltransferase and histone deacetylase, respectively. In addition, methylation-specific PCR analysis revealed increased HHIP promoter methylation in Cr(VI)-transformed cells. Moreover, the enrichments of several histone marks were altered in HHIP promoter region to facilitate a repressed chromatin domain. These results are consistent with our previous findings that Cr(VI) is capable of inducing a broad range of changes in the epigenetic machinery (41). In human lung adenocarcinoma A549 cells, Cr(VI) exposure altered histone methylation in both global and gene promoter-specific manner and repressed DNA mismatch repair (hMLH1) transcription (41). Furthermore, lung cancers from chromate workers exhibited increased promoter hypermethylation of MLH1 compared with non-chromate-related lung cancers (42–44). Lastly, HHIP promoter hypermethylation has been reported in many human cancers, including lung cancers, accompanied with HHIP silencing (19,21,24,25,45). Re-expressing HHIP in gastric cancers and lung cancers resulted in reduced cell proliferation, migration and invasion (19,20,37). Taken together, epigenetic silencing of HHIP contributes to Cr(VI)-induced malignant transformation and tumor progression.

In conclusion, the present study elucidated a new mechanism by which Cr(VI) exposure downregulated HHIP expression, leading to aberrant activation of Hh signaling. This, in turn, facilitated cell proliferation and anchorage-independent growth and promoted malignant transformation of human lung cells. Our study is the first to link Cr(VI) exposure to the dysregulation of Hh signaling in malignant transformation and lung carcinogenesis. These findings not only improve our understanding of the changes in the Hh signaling cascade following Cr(VI) exposure but also provide new insights for developing a better diagnostic and prognostic strategy for Cr(VI)-related human lung cancer.

Supplementary material

Supplementary data are available at *Carcinogenesis* online.

Funding

This work was supported, in part, by the National Institutes of Environmental Health Sciences (NIEHS) (R03ES023028 to H.S., P30ES000260 to H.S., M.C.).

Conflict of Interest Statement: The authors declare no conflict of interest.

References

1. Siegel, R.L. *et al.* (2020) Cancer statistics, 2020. *CA. Cancer J. Clin.*, 70, 7–30.
2. Herbst, R.S. *et al.* (2018) The biology and management of non-small cell lung cancer. *Nature*, 553, 446–454.
3. Holmes, A.L. *et al.* (2008) Carcinogenicity of hexavalent chromium. *Indian J. Med. Res.*, 128, 353–372.
4. Costa, M. *et al.* (2006) Toxicity and carcinogenicity of chromium compounds in humans. *Crit. Rev. Toxicol.*, 36, 155–163.
5. Gibb, H.J. *et al.* (2000) Lung cancer among workers in chromium chemical production. *Am. J. Ind. Med.*, 38, 115–126.
6. Park, R.M. *et al.* (2004) Hexavalent chromium and lung cancer in the chromate industry: a quantitative risk assessment. *Risk Anal.*, 24, 1099–1108.
7. IARC. (1990) Chromium, nickel and welding. *IARC Monogr Eval Carcinog Risks Hum*, 49, 1–648.
8. Sun, H. *et al.* (2015) Oral chromium exposure and toxicity. *Curr. Environ. Health Rep.*, 2, 295–303.
9. Chen, Q.Y. *et al.* (2019) Molecular and epigenetic mechanisms of Cr(VI)-induced carcinogenesis. *Toxicol. Appl. Pharmacol.*, 377, 114636.
10. Sun, H. *et al.* (2011) Comparison of gene expression profiles in chromate transformed BEAS-2B cells. *PLoS One*, 6, e17982.
11. Varjosalo, M. *et al.* (2008) Hedgehog: functions and mechanisms. *Genes Dev.*, 22, 2454–2472.
12. Pak, E. *et al.* (2016) Hedgehog signal transduction: key players, oncogenic drivers, and cancer therapy. *Dev. Cell*, 38, 333–344.
13. Petrov, K. *et al.* (2017) Sending and receiving hedgehog signals. *Annu. Rev. Cell Dev. Biol.*, 33, 145–168.
14. Chuang, P.T. *et al.* (1999) Vertebrate Hedgehog signalling modulated by induction of a Hedgehog-binding protein. *Nature*, 397, 617–621.
15. Velcheti, V. *et al.* (2007) Hedgehog signaling pathway and lung cancer. *J. Thorac. Oncol.*, 2, 7–10.
16. Yuan, Z. *et al.* (2007) Frequent requirement of hedgehog signaling in non-small cell lung carcinoma. *Oncogene*, 26, 1046–1055.
17. Watkins, D.N. *et al.* (2003) Hedgehog signalling within airway epithelial progenitors and in small-cell lung cancer. *Nature*, 422, 313–317.
18. Hong, Z. *et al.* (2014) Activation of hedgehog signaling pathway in human non-small cell lung cancers. *Pathol. Oncol. Res.*, 20, 917–922.
19. Lin, E.H. *et al.* (2016) Hedgehog pathway maintains cell survival under stress conditions, and drives drug resistance in lung adenocarcinoma. *Oncotarget*, 7, 24179–24193.
20. Zhao, J.G. *et al.* (2019) HHIP overexpression inhibits the proliferation, migration and invasion of non-small cell lung cancer. *PLoS One*, 14, e0225755.
21. Shahi, M.H. *et al.* (2011) Human hedgehog interacting protein expression and promoter methylation in medulloblastoma cell lines and primary tumor samples. *J. Neurooncol.*, 103, 287–296.
22. Eichenmüller, M. *et al.* (2009) Blocking the hedgehog pathway inhibits hepatoblastoma growth. *Hepatology*, 49, 482–490.
23. Tada, M. *et al.* (2008) Down-regulation of hedgehog-interacting protein through genetic and epigenetic alterations in human hepatocellular carcinoma. *Clin. Cancer Res.*, 14, 3768–3776.
24. Taniguchi, H. *et al.* (2007) Transcriptional silencing of hedgehog-interacting protein by CpG hypermethylation and chromatic structure in human gastrointestinal cancer. *J. Pathol.*, 213, 131–139.
25. Martin, S.T. *et al.* (2005) Aberrant methylation of the Human Hedgehog interacting protein (HHIP) gene in pancreatic neoplasms. *Cancer Biol. Ther.*, 4, 728–733.
26. Song, Y. *et al.* (2013) Altered expression of PTCH and HHIP in gastric cancer through their gene promoter methylation: novel targets for gastric cancer. *Mol. Med. Rep.*, 7, 1159–1168.
27. Song, Y. *et al.* (2014) Occurrence of HHIP gene CpG island methylation in gastric cancer. *Oncol. Lett.*, 8, 2340–2344.
28. Ingham, P.W. *et al.* (2011) Mechanisms and functions of Hedgehog signalling across the metazoa. *Nat. Rev. Genet.*, 12, 393–406.
29. Kiprilov, E.N. *et al.* (2008) Human embryonic stem cells in culture possess primary cilia with hedgehog signaling machinery. *J. Cell Biol.*, 180, 897–904.
30. Bangs, F. *et al.* (2017) Primary cilia and mammalian hedgehog signaling. *Cold Spring Harb. Perspect Biol.*, 9, a028175.
31. Spektor, A. *et al.* (2007) Cep97 and CP110 suppress a cilia assembly program. *Cell*, 130, 678–690.
32. Ishikawa, Y. *et al.* (1994) Characteristics of chromate workers' cancers, chromium lung deposition and precancerous bronchial lesions: an autopsy study. *Br. J. Cancer*, 70, 160–166.
33. Savani, M. *et al.* (2012) Sonic hedgehog pathway expression in non-small cell lung cancer. *Ther. Adv. Med. Oncol.*, 4, 225–233.
34. Gialmanidis, I.P. *et al.* (2009) Overexpression of hedgehog pathway molecules and FOXM1 in non-small cell lung carcinomas. *Lung Cancer*, 66, 64–74.
35. Jiang, W.G. *et al.* (2015) Expression of Sonic Hedgehog (SHH) in human lung cancer and the impact of YangZheng XiaoJi on SHH-mediated biological function of lung cancer cells and tumor growth. *Anticancer Res.*, 35, 1321–1331.

36. Yang, Q. *et al.* (2012) STAT3 activation and aberrant ligand-dependent sonic hedgehog signaling in human pulmonary adenocarcinoma. *Exp. Mol. Pathol.*, 93, 227–236.
37. Zuo, Y. *et al.* (2018) Inhibition of HHIP promoter methylation suppresses human gastric cancer cell proliferation and migration. *Cell. Physiol. Biochem.*, 45, 1840–1850.
38. Sun, H. *et al.* (2018) Hedgehog interacting protein 1 is a prognostic marker and suppresses cell metastasis in gastric cancer. *J. Cancer*, 9, 4642–4649.
39. Mori, S. *et al.* (2009) Anchorage-independent cell growth signature identifies tumors with metastatic potential. *Oncogene*, 28, 2796–2805.
40. Cifone, M.A. *et al.* (1980) Correlation of patterns of anchorage-independent growth with *in vivo* behavior of cells from a murine fibrosarcoma. *Proc. Natl. Acad. Sci. U. S. A.*, 77, 1039–1043.
41. Sun, H. *et al.* (2009) Modulation of histone methylation and MLH1 gene silencing by hexavalent chromium. *Toxicol. Appl. Pharmacol.*, 237, 258–266.
42. Ali, A.H. *et al.* (2011) Aberrant DNA methylation of some tumor suppressor genes in lung cancers from workers with chromate exposure. *Mol. Carcinog.*, 50, 89–99.
43. Tsuboi, M. *et al.* (2020) Chromate exposure induces DNA hypermethylation of the mismatch repair gene MLH1 in lung cancer. *Mol. Carcinog.*, 59, 24–31.
44. Takahashi, Y. *et al.* (2005) Microsatellite instability and protein expression of the DNA mismatch repair gene, hMLH1, of lung cancer in chromate-exposed workers. *Mol. Carcinog.*, 42, 150–158.
45. Shahi, M.H. *et al.* (2015) Epigenetic regulation of human hedgehog interacting protein in glioma cell lines and primary tumor samples. *Tumour Biol.*, 36, 2383–2391.